# Mixed and Nitsche's discretizations of frictional contact-mechanics in fractured porous media

Laurence Beaude, Franz Chouly, Mohamed Laaziri, Roland Masson

# Mixed and Nitsche's discretizations of frictional contact-mechanics in fractured porous media

L. Beaude[1], F. Chouly[2], M. Laaziri[3], and R. Masson[4]

[1] BRGM, Orléans, laurence.beaude@brgm.fr
[2] Université de Bourgogne, Institut de Mathématiques de Bourgogne, 21078 Dijon, France – Center for Mathematical Modeling and Department of Mathematical Engineering, University of Chile and IRL 2807 – CNRS, Santiago, Chile – Departamento de Ingeniería Matemática, CI$^2$MA, Universidad de Concepción, Casilla 160-C, Concepción, Chile, franz.chouly@u-bourgogne.fr
[3] Université Côte d'Azur, Inria, CNRS, LJAD, UMR 7351 CNRS, team Coffee, Parc Valrose 06108 Nice Cedex 02, France, mohamed.laaziri@univ-cotedazur.fr
[4] Université Côte d'Azur, Inria, CNRS, LJAD, UMR 7351 CNRS, team Coffee, Parc Valrose 06108 Nice Cedex 02, France, roland.masson@univ-cotedazur.fr

**Abstract.** This work deals with the discretization of single-phase Darcy flows in fractured and deformable porous media, including frictional contact at the matrix-fracture interfaces. Fractures are described as a network of planar surfaces leading to so-called mixed-dimensional models. Small displacements and a linear poro-elastic behavior are considered in the matrix. One key difficulty to simulate such coupled poro-mechanical models is related to the formulation and discretization of the contact mechanical sub-problem. Our starting point is based on the mixed formulation using facewise constant Lagrange multipliers along the fractures representing normal and tangential stresses. This is a natural choice for the discretization of the contact dual cone in order to account for complex fracture networks with corners and intersections. It leads to local expressions of the contact conditions and to efficient semi-smooth nonlinear solvers. On the other hand, such a mixed formulation requires to satisfy a compatibility condition between the discrete spaces restricting the choice of the displacement space and potentially leading to sub-optimal accuracy. This motivates the investigation of two alternative formulations based either on a stabilized mixed formulation or on the Nitsche's method. These three types of formulations are first investigated theoritically in order to enhance their connections. Then, they are compared numerically in terms of accuracy and nonlinear convergence on a coupled poromechanical model.

**Keywords:** Contact mechanics · Coulomb friction · Stabilized mixed method · Nitsche's method · Poromechanics · Discrete Fracture Matrix model.

## 1 Mixed-dimensional contact mechanics

In what follows, scalar fields are represented by lightface letters, vector fields by boldface letters. We use the overline notation $\overline{v}$ to distinguish an exact (scalar or vector) field from its discrete counterpart $v$.

We consider a network $\Gamma$ of planar fractures $\Gamma_i$, $i \in I$ immersed in the surrounding matrix domain $\Omega \backslash \overline{\Gamma}$ with $\Omega \subset \mathbb{R}^d$, $d \in \{2, 3\}$ a bounded polytopal domain (see Figure 1).

The two sides of a given fracture of $\Gamma$ are denoted by $\pm$ in the matrix domain, with unit normal vectors $\mathbf{n}^{\pm}$ oriented outward from the sides $\pm$. We denote by $\gamma_{\mathfrak{a}}$ the trace operators on the side $\mathfrak{a} \in \{+, -\}$ of $\Gamma$ for functions in $H^1(\Omega \backslash \overline{\Gamma})$. The jump operator on $\Gamma$ for functions $\overline{\mathbf{u}}$ in $(H^1(\Omega \backslash \overline{\Gamma}))^d$ is defined by $[\![\overline{\mathbf{u}}]\!] = \gamma_+ \overline{\mathbf{u}} - \gamma_- \overline{\mathbf{u}}$, and we denote by

$$[\![\overline{\mathbf{u}}]\!]_n = [\![\overline{\mathbf{u}}]\!] \cdot \mathbf{n}^+ \quad \text{and} \quad [\![\overline{\mathbf{u}}]\!]_\tau = [\![\overline{\mathbf{u}}]\!] - [\![\overline{\mathbf{u}}]\!]_n \mathbf{n}^+$$

its normal and tangential components. The symmetric gradient operator $\mathfrak{e}$ is defined such that $\mathfrak{e}(\overline{\mathbf{v}}) = \frac{1}{2}(\nabla \overline{\mathbf{v}} + (\nabla \overline{\mathbf{v}})^t)$ for a given vector field $\overline{\mathbf{v}} \in H^1(\Omega \backslash \overline{\Gamma})^d$.

The space for the displacement field is defined by

$$\mathbf{U}_0 = \{\overline{\mathbf{v}} \in (H^1(\Omega \backslash \overline{\Gamma}))^d \,|\, \overline{\mathbf{v}} = 0 \text{ on } \partial\Omega\},$$

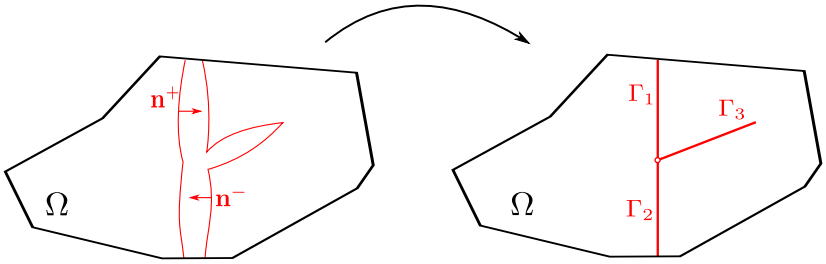


Fig. 1: Illustration of the dimension reduction in the fracture aperture for a 2D domain $\Omega$ with three intersecting fractures $\Gamma_i$, $i \in \{1,2,3\}$, with the equi-dimensional geometry on the left and the mixed-dimensional geometry on the right.

endowed with the norm $\|\overline{\mathbf{v}}\|_{\mathbf{U}_0} = \|\nabla\overline{\mathbf{v}}\|_{L^2(\Omega)^d}$. We consider a static mechanical model accounting for an isotropic linear elastic behavior in the matrix domain and a Coulomb frictional contact at the matrix–fracture interface $\Gamma$:

$$\begin{cases} -\mathrm{div}\Big(\mathfrak{o}(\overline{\mathbf{u}})\Big) = \mathbf{f} & \text{on } \Omega\backslash\overline{\Gamma}, \\ \mathfrak{o}(\overline{\mathbf{u}}) = \frac{E}{1+\nu}\Big(\mathfrak{e}(\overline{\mathbf{u}}) + \frac{\nu}{1-2\nu}(\mathrm{div}\,\overline{\mathbf{u}})\mathbb{I}\Big) & \text{on } \Omega\backslash\overline{\Gamma}, \\ \mathbf{T}^+(\overline{\mathbf{u}}) + \mathbf{T}^-(\overline{\mathbf{u}}) = \mathbf{0} & \text{on } \Gamma, \\ T_n(\overline{\mathbf{u}}) \leqslant 0,\ [\![\overline{\mathbf{u}}]\!]_n \leqslant 0,\ [\![\overline{\mathbf{u}}]\!]_n\, T_n(\overline{\mathbf{u}}) = 0 & \text{on } \Gamma, \\ |\mathbf{T}_\tau(\overline{\mathbf{u}})| \leqslant -F\ T_n(\overline{\mathbf{u}}) & \text{on } \Gamma, \\ ([\![\overline{\mathbf{u}}]\!]_\tau)\cdot\mathbf{T}_\tau(\overline{\mathbf{u}}) - F\ T_n(\overline{\mathbf{u}})|[\![\overline{\mathbf{u}}]\!]_\tau| = 0 & \text{on } \Gamma. \end{cases} \tag{1}$$

In (1), $E$ and $\nu$ are the Young modulus and Poisson ratio, $F \geqslant 0$ is the friction coefficient, and the contact tractions are defined by

$$\begin{cases} \mathbf{T}^{\mathfrak{a}}(\overline{\mathbf{u}}) = \mathfrak{o}(\overline{\mathbf{u}})\mathbf{n}^{\mathfrak{a}},\ \mathfrak{a} \in \{+,-\}, \quad \mathbf{T}(\overline{\mathbf{u}}) = \mathbf{T}^+(\overline{\mathbf{u}}), \\ T_n(\overline{\mathbf{u}}) = \mathbf{T}(\overline{\mathbf{u}})\cdot\mathbf{n}^+, \quad \mathbf{T}_\tau(\overline{\mathbf{u}}) = \mathbf{T}(\overline{\mathbf{u}}) - (\mathbf{T}(\overline{\mathbf{u}})\cdot\mathbf{n}^+)\mathbf{n}^+. \end{cases}$$

## 2 Mixed, stabilized mixed and Nitsche's discretizations of the contact mechanical model

Let $\mathbf{U}_h$ denote a family of Finite Element subspaces of $\mathbf{U}_0$, indexed by $h$ coming from a family of simplicial (to fix ideas) meshes $\mathcal{M}_h$ of the domain $\Omega$. The mesh $\mathcal{M}_h$ is assumed conforming to the fracture network and we denote by $\mathcal{F}_\Gamma$ the subset of faces of the mesh such that

$$\overline{\Gamma} = \bigcup_{\sigma\in\mathcal{F}_\Gamma} \overline{\sigma}.$$

The family of meshes $\mathcal{M}_h$ is assumed to be shape regular in the sense that the shape regularity parameter $S_R = \max_h \max_{K\in\mathcal{M}_h} \frac{h_K}{\rho_K}$ is bounded, where $h_K$ denotes the diameter of the cell $K$ and $\rho_K$ is the radius of the inscribed ball in $K$.

The subspace $M_h \subset L^2(\Gamma)$ denotes the set of piecewise constant functions on the partition $\mathcal{F}_\Gamma$ and we set $\mathbf{M}_h = (M_h)^d$. For $\boldsymbol{\lambda}$ in $\mathbf{M}_h$, we will use the decomposition $\boldsymbol{\lambda} = (\lambda_n, \boldsymbol{\lambda}_\tau)$ with $\lambda_n = \boldsymbol{\lambda}\cdot\mathbf{n}^+$, $\boldsymbol{\lambda}_\tau = \boldsymbol{\lambda} - \lambda_n\mathbf{n}^+$, and identify $\boldsymbol{\lambda}_\tau$ to an element of $(M_h)^{d-1}$ based on an orthogonal basis local to each planar fracture. We denote by $\boldsymbol{\lambda}_\sigma$ the constant value of $\boldsymbol{\lambda} \in \mathbf{M}_h$ on the face $\sigma \in \mathcal{F}_\Gamma$ and by $\lambda_{n,\sigma}$ and $\boldsymbol{\lambda}_{\tau,\sigma}$ its normal and tangential components. The orthogonal projection from $L^2(\Gamma)$ to $M_h$ is denoted by $\pi^0_{\mathcal{F}}$. By abuse of notations, the same notation will be used for the orthogonal projection from $(L^2(\Gamma))^d$ to $\mathbf{M}_h$. For a face $\sigma \in \mathcal{F}_\Gamma$, the face average projection

will be denoted by $\pi_\sigma^0$ in both cases.

The following notations will be used. For all $x \in \mathbb{R}$, we set

$$[x]_{\mathbb{R}^-} = \min(0, x), \quad [x]_{\mathbb{R}^+} = \max(0, x) = -[-x]_{\mathbb{R}^-}.$$

For all $\mathbf{x} \in \mathbb{R}^{d-1}$ and $\alpha \geqslant 0$, we denote by $[\mathbf{x}]_\alpha$ the orthogonal projection of $\mathbf{x}$ on the ball $\mathcal{B}(\mathbf{0}, \alpha) \subset \mathbb{R}^{d-1}$ where $\mathcal{B}(\mathbf{0}, \alpha)$ is the closed ball of origin $\mathbf{0}$ and radius $\alpha$, such that

$$[\mathbf{x}]_\alpha = \begin{cases} \mathbf{x} & \text{if } |\mathbf{x}| \leqslant \alpha, \\ \alpha \frac{\mathbf{x}}{|\mathbf{x}|} & \text{else .} \end{cases}$$

**Mixed formulation**: this work focuses on mixed formulations using facewise constant Lagrange multipliers, which can handle fracture intersections, corners, and tips and facilitate the expression of discrete contact conditions and semi-smooth Newton solvers. However, these formulations require assuming the uniform inf-sup condition between the space of displacement fields and the space of Lagrange multipliers $\mathbf{U}_h \times \mathbf{M}_h$ (see e.g. [6]). There exists $c_\star$ independent on the mesh such that

$$\inf_{\boldsymbol{\mu} \in \mathbf{M}_h} \sup_{\mathbf{v} \in \mathbf{U}_h} \frac{\displaystyle\int_\Gamma \boldsymbol{\mu} \cdot [\![\mathbf{v}]\!] d\sigma}{\|\mathbf{v}\|_{\mathbf{U}_0} \|\boldsymbol{\mu}\|_{H^{-\frac{1}{2}}(\Gamma)^d}} \geqslant c_\star > 0. \tag{2}$$

Let us define the discrete dual cone of normal Lagrange multipliers as

$$\Lambda_h = \{\lambda_n \in M_h \,|\, \lambda_n \geqslant 0 \text{ on } \Gamma\},$$

and the discrete dual cone of vectorial Lagrange multipliers given $\lambda_n \in \Lambda_h$ as

$$\boldsymbol{\Lambda}_h(\lambda_n) = \{\boldsymbol{\mu} = (\mu_n, \boldsymbol{\mu}_\tau) \in \mathbf{M}_h \,|\, \mu_n \geqslant 0, |\boldsymbol{\mu}_\tau| \leqslant F\lambda_n \text{ on } \Gamma\}.$$

Note that the friction coefficient will be assumed to be facewise constant on the partition $\mathcal{F}_\Gamma$. The mixed discretization of the static contact mechanical model reads: find $(\mathbf{u}, \boldsymbol{\lambda} = (\lambda_n, \boldsymbol{\lambda}_\tau)) \in \mathbf{U}_h \times \boldsymbol{\Lambda}_h(\lambda_n)$ such that

$$\begin{cases} \displaystyle\int_\Omega \mathfrak{o}(\mathbf{u}) : \mathfrak{c}(\mathbf{v}) \mathrm{d}\mathbf{x} + \int_\Gamma \boldsymbol{\lambda} \cdot [\![\mathbf{v}]\!] d\sigma = \int_\Omega \mathbf{f} \cdot \mathbf{v} \, \mathrm{d}\mathbf{x}, \\ \displaystyle\int_\Gamma (\boldsymbol{\mu} - \boldsymbol{\lambda}) \cdot [\![\mathbf{u}]\!] d\sigma \leqslant 0, \end{cases} \tag{3}$$

for all $(\mathbf{v}, \boldsymbol{\mu}) \in \mathbf{U}_h \times \boldsymbol{\Lambda}_h(\lambda_n)$.

Note that the variational inequality in (3) is equivalent to the following equations for each $\sigma \in \mathcal{F}_\Gamma$

$$\lambda_{n,\sigma} - [\lambda_{n,\sigma} + \beta_n^{\mathrm{sm}} \pi_\sigma^0 [\![\mathbf{u}]\!]_n]_{\mathbb{R}^+} = 0, \quad \boldsymbol{\lambda}_{\tau,\sigma} - [\boldsymbol{\lambda}_{\tau,\sigma} + \beta_\tau^{\mathrm{sm}} \pi_\sigma^0 [\![\mathbf{u}]\!]_\tau]_{F_\sigma [\lambda_{n,\sigma} + \beta_n^{\mathrm{sm}} \pi_\sigma^0 [\![\mathbf{u}]\!]_n]_{\mathbb{R}^+}} = 0, \tag{4}$$

with $\beta_n^{\mathrm{sm}} > 0$, $\beta_\tau^{\mathrm{sm}} > 0$, which are the basis of the semi-smooth Newton algorithm used in the numerical section for the solution of the mixed discretization.

**Stabilized mixed and Mean-Nitsche's formulations**: in order to circumvent the inf-sup condition (2), we consider in this subsection the following stabilized mixed formulation in the spirit of [5]. Exploiting their facewise constant approximation, the Lagrange multipliers can be eliminated leading to a Nitsche's type discretization with face averaging. It results that this stabilized mixed formulation can also be useful when $\mathbf{U}_h \times \mathbf{M}_h$ satisfies the inf-sup condition in order to eliminate the Lagrange multipliers. In that case, we can prove that the stabilized mixed solution converges to the mixed solution at the limit of large stabilization parameters.

Let us fix a parameter $\theta \in \mathbb{R}$ and two non-negative functions $\beta_n$ and $\beta_\tau$ on $\Gamma$ typically set to $\frac{\beta_n^0}{h_\sigma}$ and $\frac{\beta_\tau^0}{h_\sigma}$ on each face $\sigma$ of $\Gamma$, where $h_\sigma$ is the diameter of the face $\sigma$. By abuse of notations, in

the following, $h$ will also denote the facewise constant function of $L^2(\Gamma)$ with value $h_\sigma$ on each face $\sigma \in \mathcal{F}_\Gamma$. The stabilized mixed discretization of the static contact mechanical model reads: find $(\mathbf{u}, \boldsymbol{\lambda} = (\lambda_n, \boldsymbol{\lambda}_\tau)) \in \mathbf{U}_h \times \boldsymbol{\Lambda}_h(\lambda_n)$ such that

$$\begin{cases} \displaystyle\int_\Omega \Big(\mathfrak{o}(\mathbf{u}) : \mathfrak{e}(\mathbf{v}) - b\,\overline{p}_m \mathrm{div}(\mathbf{v})\Big)\mathrm{d}\mathbf{x} + \int_\Gamma \boldsymbol{\lambda}\cdot[\![\mathbf{v}]\!]d\sigma + \int_\Gamma \overline{p}_f\,[\![\mathbf{v}]\!]_n\,\mathrm{d}\sigma \\ \displaystyle -\int_\Gamma \frac{\theta}{\beta_n}(\lambda_n + T_n(\mathbf{u}))\pi^0_{\mathcal{F}} T_n(\mathbf{v})d\sigma - \int_\Gamma \frac{\theta}{\beta_\tau}(\boldsymbol{\lambda}_\tau + \mathbf{T}_\tau(\mathbf{u}))\cdot\pi^0_{\mathcal{F}}\mathbf{T}_\tau(\mathbf{v})d\sigma = \int_\Omega \mathbf{f}\cdot\mathbf{v}\,\mathrm{d}\mathbf{x}, \\ \displaystyle\int_\Gamma (\boldsymbol{\mu}-\boldsymbol{\lambda})\cdot[\![\mathbf{u}]\!]d\sigma \\ \displaystyle -\int_\Gamma \frac{1}{\beta_n}(\mu_n-\lambda_n)(\lambda_n + T_n(\mathbf{u}))d\sigma - \int_\Gamma \frac{1}{\beta_\tau}(\boldsymbol{\mu}_\tau-\boldsymbol{\lambda}_\tau)\cdot(\boldsymbol{\lambda}_\tau+\mathbf{T}_\tau(\mathbf{u}))d\sigma \leqslant 0, \end{cases} \tag{5}$$

for all $(\mathbf{v}, \boldsymbol{\mu}) \in \mathbf{U}_h \times \boldsymbol{\Lambda}_h(\lambda_n)$.

Thanks to their facewise constant approximations, the Lagrange multipliers can be eliminated from the stabilized mixed formulation using that the variational inequality in (5) with $\boldsymbol{\lambda} \in \boldsymbol{\Lambda}_h(\lambda_n)$ is equivalent to the following equations:

$$\begin{cases} -\lambda_n = [\pi^0_{\mathcal{F}}\Big(T_n(\mathbf{u}) - \beta_n[\![\mathbf{u}]\!]_n\Big)]_{\mathbb{R}^-}, \\ -\boldsymbol{\lambda}_\tau = [\pi^0_{\mathcal{F}}\Big(\mathbf{T}_\tau(\mathbf{u}) - \beta_\tau[\![\mathbf{u}]\!]_\tau\Big)]\Big(-F\Big[\pi^0_{\mathcal{F}}\Big(T_n(\mathbf{u})-\beta_n[\![\mathbf{u}]\!]_n\Big)\Big]_{\mathbb{R}^-}\Big). \end{cases} \tag{6}$$

From (6), we can eliminate the Lagrange multipliers leading to the following equivalent Nitsche's type formulation: find $\mathbf{u} \in \mathbf{U}_h$ such that

$$\begin{aligned} &\int_\Omega \mathfrak{o}(\mathbf{u}) : \mathfrak{e}(\mathbf{v})\mathrm{d}\mathbf{x} - \int_\Gamma \frac{\theta}{\beta_n} T_n(\mathbf{u})\cdot\pi^0_{\mathcal{F}} T_n(\mathbf{v})\,\mathrm{d}\sigma - \int_\Gamma \frac{\theta}{\beta_\tau}\mathbf{T}_\tau(\mathbf{u})\cdot\pi^0_{\mathcal{F}}\mathbf{T}_\tau(\mathbf{v})\,\mathrm{d}\sigma \\ &+ \int_\Gamma \frac{1}{\beta_n}\Big[\pi^0_{\mathcal{F}}\Big(T_n(\mathbf{u}) - \beta_n[\![\mathbf{u}]\!]_n\Big)\Big]_{\mathbb{R}^-}\Big(\theta T_n(\mathbf{v}) - \beta_n[\![\mathbf{v}]\!]_n\Big)\,\mathrm{d}\sigma \\ &+ \int_\Gamma \frac{1}{\beta_\tau}\Big[\pi^0_{\mathcal{F}}\Big(\mathbf{T}_\tau(\mathbf{u}) - \beta_\tau[\![\mathbf{u}]\!]_\tau\Big)\Big]\Big(-F\Big[\pi^0_{\mathcal{F}}\Big(T_n(\mathbf{u})-\beta_n[\![\mathbf{u}]\!]_n\Big)\Big]_{\mathbb{R}^-}\Big)\cdot\Big(\theta\mathbf{T}_\tau(\mathbf{v}) - \beta_\tau[\![\mathbf{v}]\!]_\tau\Big)\,\mathrm{d}\sigma \\ &= \int_\Omega \mathbf{f}\cdot\mathbf{v}\,\mathrm{d}\mathbf{x}, \end{aligned} \tag{7}$$

for all $\mathbf{v} \in \mathbf{U}_h$. Due to the face averaging, this formulation will be termed mean-Nitsche's method in the following. Note that it is not consistent in the usual Nitsche's sense since the exact solution $\overline{\mathbf{u}}$ does not satisfy (7). It is only consistent as a mixed formulation in the sense that $(\overline{\mathbf{u}}, \overline{\boldsymbol{\lambda}})$ satisfies (5).

For the Coulomb frictional model we can state the following Proposition, the proof of which can be found in [1].

**Proposition 1.** *Let $\overline{\beta}^0 > 0$ be large enough. For $\beta^0 \geqslant \overline{\beta}^0$, there exists a solution $(\mathbf{u}_\beta, \boldsymbol{\lambda}_\beta) \in \mathbf{U}_h \times \boldsymbol{\Lambda}_h(\lambda_{\beta,n})$ to (7) with $\|\mathbf{u}_\beta\|_{\mathbf{U}_0} + \|h^{1/2}\boldsymbol{\lambda}_\beta\|_{L^2(\Gamma)^d} \leqslant C$, $C$ independent of $\beta^0_n, \beta^0_\tau$ and $h$ but depending on the shape regularity parameter $S_R$ and the physical data. Furthermore, any sequence of such solutions with $\beta^0$ going to infinity admits a subsequence which converges to $(\mathbf{u}, \boldsymbol{\lambda}) \in \mathbf{U}_h \times \boldsymbol{\Lambda}_h(\lambda_n)$ solution of (3).*

**Nitsche's formulation**: we follow the Nitsche's formulation introduced in [4] for Coulomb frictional models. It can be obtained by dropping the face averaging operators in (7): find $\mathbf{u} \in \mathbf{U}_h$

such that for all $\mathbf{v} \in \mathbf{U}_h$, one has

$$\begin{aligned}
&\int_\Omega \Big(\mathfrak{o}(\mathbf{u}) : \mathfrak{e}(\mathbf{v})\Big)\mathrm{d}\mathbf{x} - \int_\Gamma \frac{\theta}{\beta_n} T_n(\mathbf{u}) \cdot T_n(\mathbf{v})\ \mathrm{d}\sigma - \int_\Gamma \frac{\theta}{\beta_\tau} \mathbf{T}_\tau(\mathbf{u}) \cdot \mathbf{T}_\tau(\mathbf{v})\ \mathrm{d}\sigma \\
&+ \int_\Gamma \frac{1}{\beta_n} \Big[T_n(\mathbf{u}) - \beta_n [\![\mathbf{u}]\!]_n\Big]_{\mathbb{R}^-} \Big(\theta T_n(\mathbf{v}) - \beta_n [\![\mathbf{v}]\!]_n\Big)\ \mathrm{d}\sigma \\
&+ \int_\Gamma \frac{1}{\beta_\tau} \Big[\mathbf{T}_\tau(\mathbf{u}) - \beta_\tau [\![\mathbf{u}]\!]_\tau\Big] \Big(-F\Big[T_n(\mathbf{u}) - \beta_n [\![\mathbf{u}]\!]_n\Big]_{\mathbb{R}^-}\Big) \cdot \Big(\theta \mathbf{T}_\tau(\mathbf{v}) - \beta_\tau [\![\mathbf{v}]\!]_\tau\Big)\ \mathrm{d}\sigma \\
&= \int_\Omega \mathbf{f} \cdot \mathbf{v}\ \mathrm{d}\mathbf{x},
\end{aligned} \tag{8}$$

## 3 Comparison of the Mixed and Nitsche formulations for a coupled poromechanical simulation

The objective of this section is to compare the efficiency of the Nitsche's and mixed formulations to simulate a poromechanical model coupling the quasi static contact mechanical model with a mixed-dimensional single phase incompressible flow. The flow model accounts for a Darcy flow in the porous matrix and a Poiseuilles flow along the fractures. Isotropic linear poroelastic laws are used for the matrix porosity $\overline{\phi}_m$ and the total stress tensor $\mathfrak{o}^T$:

$$\partial_t \overline{\phi}_m = b\ \mathrm{div}\, \partial_t \overline{\mathbf{u}} + \frac{1}{M} \partial_t \overline{p}_m, \quad \mathfrak{o}^T(\overline{\mathbf{u}}) = \mathfrak{o}(\overline{\mathbf{u}}) - b\ \overline{p}_m \mathbb{I},$$

where $\overline{p}_m$ is the matrix fluid pressure, $b$ is the Biot coefficient and $M$ Biot's modulus. The fracture aperture and the contact surface tractions are defined as follows, assuming that the fractures are filled by the fluid with contact at fracture asperities:

$$\overline{d}_f = d_0 - [\![\overline{\mathbf{u}}]\!]_n, \quad \mathbf{T}^{\mathfrak{a}}(\overline{\mathbf{u}}) = (\mathfrak{o}(\overline{\mathbf{u}}) - b\ \overline{p}_m \mathbb{I})\mathbf{n}^{\mathfrak{a}} + \overline{p}_f \mathbf{n}^{\mathfrak{a}},\ \mathfrak{a} \in \{+, -\},$$

where $\overline{p}_f$ is the fracture fluid pressure and $d_0$ being the fracture aperture at contact state. Let us refer to [1] for the full description of the model.

The fluid flow is discretized in space by a mixed-dimensional Hybrid Finite Volume (HFV) scheme [3]. A $\mathbb{P}_2$ Finite Element discretization of the displacement field is used which guarantees that the inf-sup condition (2) is satisfied for the $\mathbb{P}_2 - \mathbb{P}_0$ mixed formulation (3). It also ensures the stability of the pressure displacement coupling. At each time step, the coupled non-linear system is solved using a fixed-point method on the function

$$\mathbf{g}_p : p \underset{\substack{\text{Contact Mechanics}\\ \text{Solve}}}{\rightarrow} \mathbf{u} \underset{\substack{\text{Darcy}\\ \text{Solve}}}{\rightarrow} \widetilde{p},$$

with $p = (p_m, p_f)$, accelerated by a Newton–Krylov algorithm in order to obtain at convergence the fully coupled poromechanical solution. At each evaluation of the fixed point function $\mathbf{g}_p$, the Darcy linear problem at given fracture aperture and porosity is solved using a GMRes iterative solver preconditioned by AMG while the contact mechanical model at given pressure $p$ is solved using a semi-smooth Newton method. In the following experiments, the Nitsche's parameters are fixed to $\beta_n^0 = 1000$ GPa, $\beta_\tau^0 = 40$ GPa and $\theta = -1$ (see [1] for more details motivating this choice).

Our test case is taken from [2, Section 4.3] considering a $2 \times 1$ m domain including a network $\Gamma$ of six fractures $\Gamma_i$, $i \in \{1, \cdots, 6\}$, cf. Figure 2. We consider a family of uniformly refined meshes $m \in \{0, \cdots, 3\}$ with $2855 \times 4^m$ triangular cells and $88 \times 2^m$ fracture faces.

We use the same values of Young's modulus and Poisson's ratio, $E = 4$ GPa and $\nu = 0.2$, and the same set of boundary conditions as in [2], that is, the two vertical sides of the domain are free, and we impose $\mathbf{u} = \mathbf{0}$ on the bottom side and

$$\mathbf{u}(t, \mathbf{x}) = \begin{cases} [0.005\,\mathrm{m}, -0.002\,\mathrm{m}]^\top\ 4t/T & \text{if } t \leqslant T/4, \\ [0.005\,\mathrm{m}, -0.002\,\mathrm{m}]^\top & \text{otherwise,} \end{cases} \qquad \mathbf{x} \text{ on the top boundary.}$$

The friction coefficient is set to $F = 0.5$.

To fully exploit the capabilities of the HFV flow discretization, we consider the following anisotropic permeability tensor in the matrix: $\mathbb{K}_m = K_m\, \mathbf{e}_x \otimes \mathbf{e}_x + \frac{K_m}{2}\, \mathbf{e}_y \otimes \mathbf{e}_y$, $\mathbf{e}_x$ and $\mathbf{e}_y$ being the unit vectors associated with the $x$- and $y$-axes, respectively.

The permeability coefficient is set to $K_m = 10^{-15}$ m$^2$, the Biot coefficient to $b = 0.5$, the Biot modulus to $M = 10$ GPa, the dynamic viscosity to $\eta = 10^{-3}$ Pa·s. The initial matrix porosity is set to $\phi_m^0 = 0.4$ and the fracture aperture corresponding to both contact state and zero displacement field is given by $d_0(\mathbf{x}) = \delta_0 \frac{\sqrt{\arctan(aD_i(\mathbf{x}))}}{\sqrt{\arctan(a\ell_i)}}, \quad \mathbf{x} \in \Gamma_i, \quad i \in \{1, \ldots, 6\}$, where $D_i(\mathbf{x})$ is the distance from $\mathbf{x}$ to the tips of fracture $i$, $\delta_0 = 10^{-4}$ m, $a = 25$ m$^{-1}$ and $\ell_i$ is a fracture-dependent characteristic length: it is equal to $L_i/2$ ($L_i$ being the length of fracture $i$) if fracture $i$ is immersed, to $L_i$ if one of its ends lies on the boundary, and to the distance of a corner from tips, if it includes a corner.

The initial pressure in the matrix and fracture network is $p_m^0 = p_f^0 = 10^5$ Pa. Notice that the initial fracture aperture differs from $d_0$, since it is computed by solving the mechanics given the initial pressures $p_m^0$ and $p_f^0$. The final time is set to $T = 2000$ s and the time integration uses an Euler implicit scheme with a uniform time stepping and 20 time steps. Concerning boundary conditions, for the flow, all sides are assumed impervious, except the left one, on which a pressure equal to the initial value $10^5$ Pa is prescribed.

Figure 2 exhibits the contact state along the fractures at times $t = T/4$ for which the pressures reach their maximum values and at final time $t = T$ for which the pressures are almost back to their initial value as shown in Figure 3 for the matrix pressure. Given the Biot coefficient $b = 0.5$, this pressure decrease explains the switch from slip to stick state along the fractures at times larger than $T/4$. Note that the fracture pressure basically matches with the traces of the matrix pressure due to the high conductivity of the fractures. Figure 4 plots the mean aperture as a function of time for the different meshes and the mixed and Nitsche's formulations. It shows that the Nitsche's method has a better convergence in space to the reference solution. It has been checked that the solution obtained with the mean-Nitsche's formulation is almost the same than the one of the mixed solution as expected for the inf-sup stable $\mathbb{P}_2 - \mathbb{P}_0$ approximation. Other mean quantities like the mean matrix and fracture pressures and the mean porosity as functions of time do not exhibit significant differences between both formulations. At the fracture scale, as exhibited in Figure 5, the Nitsche's method is clearly more accurate than the Mixed and Mean-Nitsche's methods in singularity regions, typically near the corner of fracture 1. Finally, Figure 6 plots the total number of semi-smooth Newton iterations for the contact mechanical model as a function of time. It shows that both the Nitsche's and mean-Nitsche's methods perform rather well compared to the mixed method which is the most efficient in terms of non-linear convergence. Note that the total number of fixed point function $\mathbf{g}_p$ evaluations is the same for all methods and both meshes and is equal to 190 for 20 time steps with a tight stopping criteria of $10^{-5}$ on the relative residual.

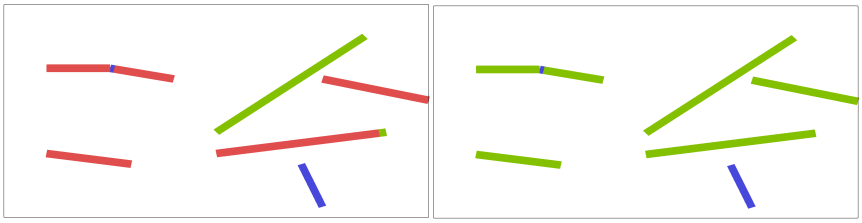

(a) (b)

Fig. 2: Contact state along the fractures (blue: open, green: stick, red: slip) for the reference solution computed on the mesh $m = 3$ at times $t = T/4$ (a) and $t = T$ (b) .

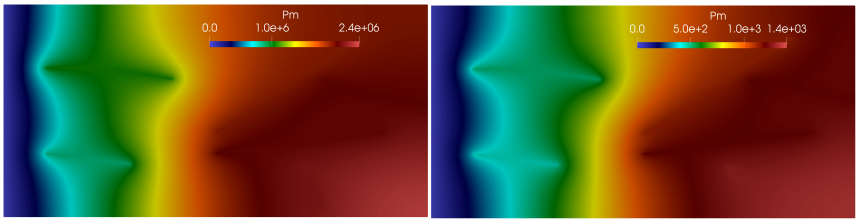


(a) (b)

Fig. 3: Matrix overpressures (compared with the initial pressure) in Pa for the reference solution computed on the mesh $m = 3$ at times $t = T/4$ (a) and $t = T$ (b) .

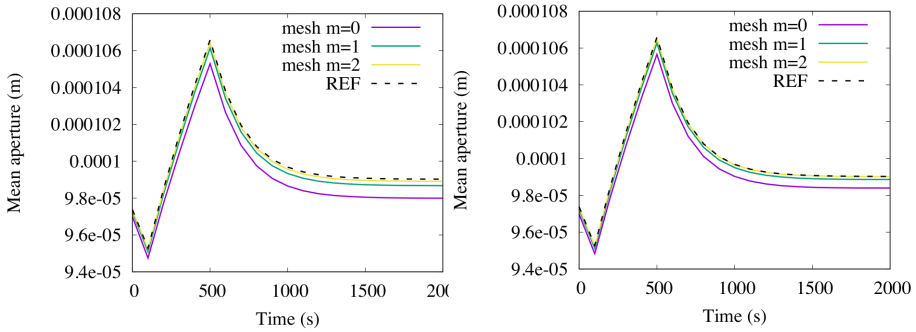


(a) (b)

Fig. 4: Mean aperture as a function of time for the mixed (a) and Nitsche's (b) formulations. The reference solution is computed using the mesh $m = 3$.

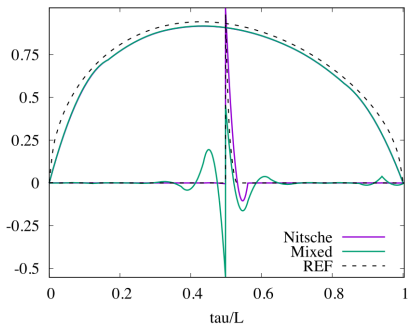


Fig. 5: Scaled normal displacement jumps at time $t = T$ for respectively fracture 1 (the upper left fracture with corner) and fracture 6 (the lower right fracture) on the coarse mesh $m = 0$ for the different discretizations (the $\mathbb{P}_2$ mean-Nitsche's basically matches with the mixed solution, hence it is not plotted).

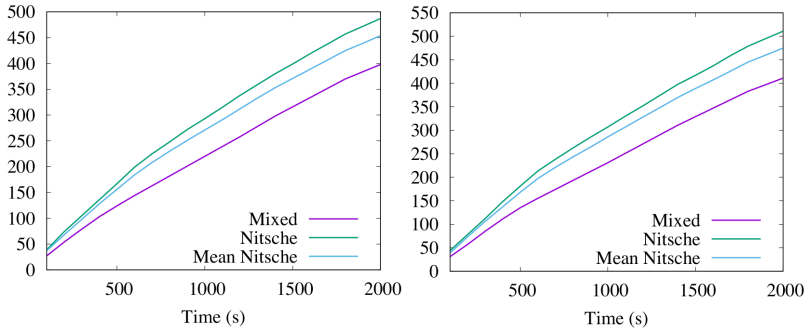


Fig. 6: Total number of semi-smooth Newton iterations for the contact mechanical model as a function of time for the mixed, Nitsche's and mean-Nitsche's formulations using the meshes $m = 0$ (a) and $m = 1$ (b).

## 4 Conclusion

This work compares the mixed formulation based on facewise constant Lagrange multipliers and the Nitsche's formulation of the Coulomb frictional contact mechanics in mixed-dimensional poroelastic models. We also introduce the mean-Nitsche's method which in some sense is shown to bridge the gap between both types of formulations. Numerical experiments show that Nitsche's method is the more accurate in singularity zones such as corners or fracture intersections. Mixed and mean-Nitsche's methods, on the other hand, are less accurate in these zones due to additional oscillations resulting from contact conditions imposed on average at each fracture face. On the other hand, the mixed method is the most robust in terms of non-linear convergence. Additional work needs to be carried out to improve the robustness of the Nitsche's method in terms of nonlinear convergence.

**Acknowledgements** the authors would like to thank BRGM and Andra for partially supporting this work and authorizing its publication. Franz Choulys work is partially supported by the I-Site BFC project NAANoD and the EIPHI Graduate School (contract ANR-17-EURE-0002). Franz Chouly is grateful of the Center for Mathematical Modeling grant FB20005.

## References

1. Beaude, L., Chouly, F., Laaziri, M., Masson, R.: Mixed and Nitsche's discretizations of Coulomb frictional contact-mechanics for mixed-dimensional poromechanical models. Preprint https://hal.science/hal-03949272 (2023)
2. Berge, R.L., Berre, I., Keilegavlen, E., Nordbotten, J.M., Wohlmuth, B.: Finite volume discretization for poroelastic media with fractures modeled by contact mechanics. International Journal for Numerical Methods in Engineering 121, 644–663, (2020)
3. Brenner, K., Hennicker, J., Masson, R., and Samier, P.: Gradient Discretization of Hybrid Dimensional Darcy Flows in Fractured Porous Media with discontinuous pressure at matrix fracture interfaces. IMA Journal of Numerical Analysis 37, 1551–1585, (2017)
4. Chouly, F., Hild, P., Lleras, V., Renard, Y.: Nitsche method for contact with Coulomb friction: existence results for the static and dynamic finite element formulations. Journal of Computational and Applied Mathematics 416 (2022)
5. Hild, P., Renard, Y.: A stabilized Lagrange multiplier method for the finite element approximation of contact problems in elastostatics. Numerische Mathematik, 115, 101–129 (2010)
6. Wohlmuth, B.: Variationally consistent discretization schemes and numerical algorithms for contact problems. Acta Numerica, 20, 569–734 (2011)